Adiabatic Pathways in the Conformational and Geometrical Photoisomerizations of the 1,2-Distyrylbenzene Isomers

G. Bartocci, S. Ciorba, U. Mazzucato, and A. Spalletti*

Dipartimento di Chimica, Università di Perugia, I-06123 Perugia, Italy

Received: April 27, 2009

The photophysical behavior of the geometrical isomers of 1,2-distyrylbenzene (1,2-DSB) has been investigated as a function of temperature by stationary and pulsed fluorimetric techniques in a nonpolar solvent. The temperature effect on the spectral properties, fluorescence quantum yields, and decay profiles allowed the role played by the conformational isomers of these molecules in the relaxation processes of the lowest excited states to be clarified. In the case of the EE geometrical isomer, a conformer (or rotamer) re-equilibration, implying an adiabatic interconversion during the lifetime in the S_1 state, was found to be operative. The deactivation channels of the excited cis isomers (ZE and ZZ) markedly depend on the conformational geometry, which is responsible for the adiabatic (rotamer-specific) cis → trans photoisomerization. The radiative and radiationless relaxation rate parameters of the isomers and conformers of 1,2-DSB, derived from the experimental and calculation results, allowed a complete and reasonably quantitative description of their behavior in the S_1 state.

1. Introduction

The photobehavior of 1,*n*-distyrylbenzenes [1,*n*-DSB, with $n = 2$, 3, or 4] has received wide attention because delocalization of the π electrons in their electronically excited states can induce new and specific properties, which can find potential applications in the field of material science, particularly in optoelectronics.[1,2]

The photophysical and photochemical behavior of *all-trans* (EE) geometrical isomers of 1,*n*-DSB bearing the two styryl substituents in the para ($n = 4$, linear conjugation)[3−6] and meta ($n = 3$, crossed conjugation)[7−10] positions has been particularly investigated in the last decades. Both series of compounds show a very small trans → cis photoisomerization yield, while the radiative relaxation is predominant. In these compounds, conformational equilibria are present in the ground state (S_0), and their role on the deactivation channels of the excited states has been investigated.[3−8,10−14]

On the contrary, the nonconjugated ortho positional isomer ($n = 2$, 1,2-DSB) has been relatively less investigated from the photophysical point of view.[9,11,12,15,16] The results have shown that the lack of conjugation markedly affects the properties of this molecule in the excited states. In fact, in fluid solution at room temperature, the main relaxation pathway of all of the geometrical isomers (EE, ZE, and ZZ) of 1,2-DSB seemed to be internal conversion (IC). The ZE and ZZ isomers photoisomerize by a predominant adiabatic pathway (a "one photon-two bonds" process is also operative for ZZ),[16] and an unexpected cyclization photoproduct was obtained exciting the EE isomer. This cyclized compound can only originate from the compressed conformation (Chart 1), which is the less stable, practically absent in the ground state, as suggested by calculations.[15] This led us to suppose that the EE rotamers could play a relevant role in the excited state deactivation also in the case of 1,2-DSB, despite the fact that only the elongated conformer is practically present in S_0.

The aim of this Article is to prove the unusual presence of very fast adiabatic interconversion processes among the rotamers during their S_1 lifetime as well as the involvement of rotamer-specific adiabatic pathways in the cis → trans photoisomerization. Therefore, a detailed study on the spectral trends and photophysical properties of the three geometrical isomers of 1,2-DSB as a function of the excitation wavelength (λ_{exc}) and temperature was carried out in a nonpolar solvent. The derived rate constants for the competitive relaxation pathways of the lowest excited singlet state of all of the conformational and geometrical isomers allowed a reasonable mechanism for the photophysical and photochemical behavior of 1,2-DSB to be proposed. The occurrence of both rotamer re-equilibration in S_1 and rotamer-specific adiabatic cis → trans isomerization confirms the relevant role of conformation in the relaxation processes of these molecules in the excited state.

2. Experimental Section

The compounds investigated were synthesized for previous works.[9] The solvent was a mixture of methylcyclohexane and 3-methylpentane (MCH/3MP, 9/1 (v/v)) from Fluka, spectrophotometric grade, further purified by standard procedure. A few measurements were also carried out in pentane/heptane (P/Hept, 1:1 (v/v)) from Aldrich.

A Perkin-Elmer Lambda 800 spectrophotometer was used for the absorption measurements.

The fluorescence spectra were obtained by a Spex Fluorog-2 F 112 AT spectrofluorimeter, using dilute solutions (absorbance <0.1 at λ_{exc}). 9,10-Diphenylanthracene in cyclohexane ($\phi_F = 0.90$, in deareated solutions[17]) was used as fluorimetric standard.

Fluorescence lifetimes (τ_F) were measured by an Edinburg Instrument 199 S spectrofuorimeter equipped with pulsed lamps, filled by N_2 or H_2, by use of the single photon counting method.

Cryostats (Oxford Instruments DN 1704 and Cryomech ST405) were used to control temperature in the 8−360 K range. For measurements as a function of temperature, the fluorescence quantum yield (ϕ_F) value at room temperature was used as reference, taking into account the changes in absorbance and refractive index with temperature.

* Corresponding author. E-mail: faby@unipg.it.

10.1021/jp903851x CCC: $40.75
Published on Web 07/06/2009

CHART 1: Conformational Equilibria of the Geometrical Isomers (EE, ZE, and ZZ) of 1,2-DSB

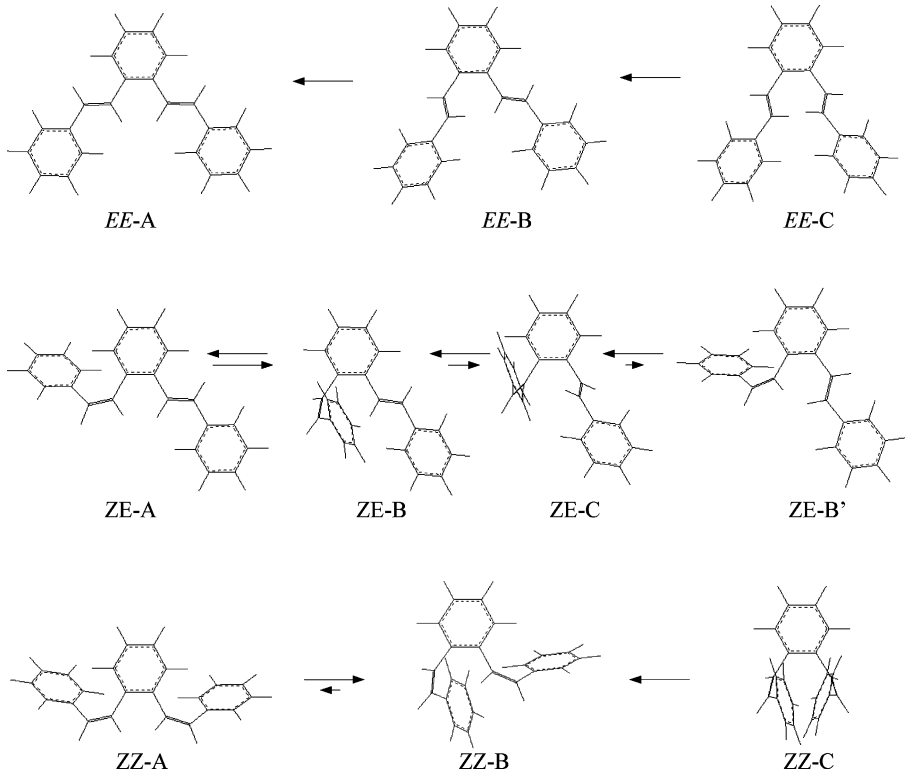

All measurements were carried out in deaerated solutions by purging with nitrogen.

The parameters reported in the tables are averages of at least three independent experiments with mean deviations of ca. 7%, 10%, and 20% for ϕ_F, τ_F, and derived parameters, respectively.

The theoretical calculations were performed using the HyperChem computational package (version 6.1): the heats of formation and dihedral angles between the ethenic bridge and the central aromatic ring were obtained for geometries optimized by the PM3 method. The electronic spectra (transition energy and oscillator strength) were calculated by ZINDO/S.

3. Results and Discussion

In principle, each of the three geometrical isomers (EE, ZE, and ZZ) of 1,2-DSB could exist in fluid solution at room temperature as a mixture of rotamers, originated by rotation of the styryl moieties around the quasi-single bond with the central benzene ring in the ground state. These conformers could have different spectral properties, as generally evidenced for diarylethenes by λ_{exc} effects on the emission spectrum and poly exponential fluorescence decay.[18,19]

In the case of the EE isomer, the calculation results (Table 1) showed that the conformational equilibrium in the ground state is almost completely shifted toward the most stable elongated conformer (A) for steric reasons. In fact, the strong deviation of the styryl groups from planarity in the semicompressed and compressed geometries (B and C rotamers, respectively, dihedral angles $\approx 40°$) decreases their stability as compared to that of the elongated species (enthalpy differences of 11.59 and 19.20 kJ mol^{-1} for B and C, respectively) and points to a negligible abundance of these two species (<1% at room temperature).[15]

On the contrary, the calculations showed that the conformational isomers of both ZE and ZZ are less different in geometry (see values of dihedral angles and formation enthalpy of Table 1); therefore, a mixture of rotamers is expected in the S_0 state for the isomers with cis double bonds. At 293 K, a relative

TABLE 1: Calculated Spectral Properties, Heats of Formations (ΔH_f^0), and Dihedral Angles between the Styryl Moieties and the Central Ring for the Elongated (A) and Compressed (B and C) Rotamers of the Geometrical Isomers of 1,2-DSB

isomer	rotamer	angles (deg)	ΔH_f^0 (kJ/mol)	λ (nm)	f
EE[a]	A	−0.34/0.88	414.72	334	1.11
				284	1.00
	B	8.57/33.49	426.31	330	0.73
				278	1.55
	C	46.56/45.91	433.92	329	0.34
				302	0.21
				272	1.11
ZE	A[b]	−39.40/10.21	434.22	316	1.04
				305	0.17
				280	0.23
				278	0.30
	B	72.08/−36.05	435.01	293	0.59
				286	0.31
				250	0.42
	C	93.18/−66.07	437.10	278	0.028
				260	0.65
				235	0.50
	B′	−51.21/−37.69	439.11	307	0.66
				295	0.18
				268	0.65
ZZ	A	50.99/−41.64	451.73	293	0.01
				283	0.51
				247	0.48
	B[b]	−60.15/−85.92	445.21	282	0.01
				267	0.57
				235	0.17
	C	−70.23/−67.38	457.25	284	0.05
				262	0.52
				251	0.23

[a] From ref 9. [b] From ref 16.

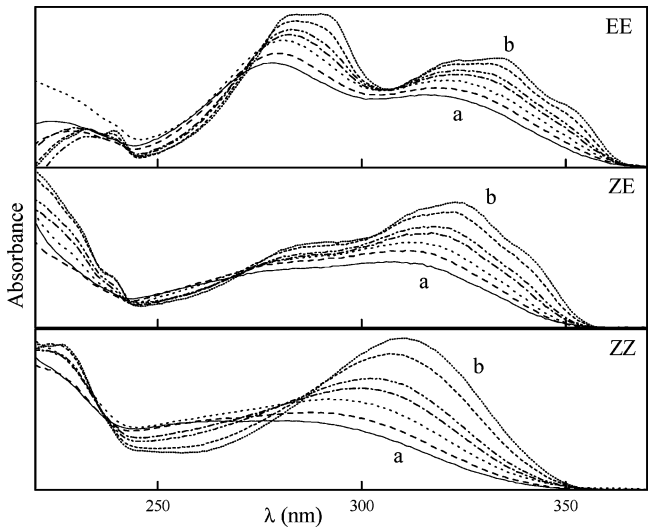

Figure 1. Spectral evolution of the absorption of the geometrical isomers of 1,2-DSB in MCH/3MP as a function of temperature from 350 K (a) to 83 K (b).

abundance of 49%, 36%, and 15% for the A, B, and C rotamers of ZE, respectively, and 6%, 92%, and 2% for the A, B, and C of ZZ, respectively, can be estimated. Chart 1 shows the most stable conformations of EE, ZE, and ZZ, as predicted by calculations.

3.1. Spectral Behavior. The absorption spectra of the EE, ZE, and ZZ isomers as a function of temperature in MCH/3MP are shown in Figure 1. The spectra measured at room temperature are reasonably well described by the theoretical calculations, as already stated in a previous work.[16]

On decreasing temperature, the absorption spectra became more structured (with a different intensity distribution of the vibronic components, particularly in the case of EE and ZE) and shifted toward the red.

This behavior, characteristic of many flexible molecules,[20−22] has been explained on the basis of excitation of sets of different ground-state species, more or less deviating from the equilibrium conformational geometry.[20] Furthermore, the ratio between the intensities at the maximum of the first and second absorption bands of ZE and ZZ markedly decreased on increasing the temperature in the range 83−350 K (from 1.48 to 1.08 for ZE and from 4 to 1 for ZZ), whereas no effect was observed in the case of EE. This is clear experimental evidence of the presence of a conformer mixture in S_0 for the cis isomers only, in agreement with the calculation results.

Figure 2 shows the fluorescence emission spectra obtained under irradiation of the three geometrical isomers in MCH/3MP at room temperature together with their absorption spectra. Under irradiation of ZE and ZZ, the emission spectrum overlapped that of EE, but only the excitation spectrum of EE overlapped the corresponding absorption spectrum. Furthermore, as already reported,[16] no effect of λ_{exc} and emission wavelength (λ_{em}) on the shape of the fluorescence emission and excitation spectra, respectively, was found. These results can be considered as an important proof of the presence of adiabatic pathways in the cis → trans photoisomerization of the ZE and ZZ isomers of 1,2-DSB in the S_1 state.[16]

The temperature effect on the spectral behavior of the three stereoisomers was quite informative. In fact, for EE the excitation spectrum is independent of λ_{em} and overlaps the absorption spectrum at all temperatures (as expected when only one species is present in S_0), whereas the emission spectrum moves with temperature, as shown in Figure 3.

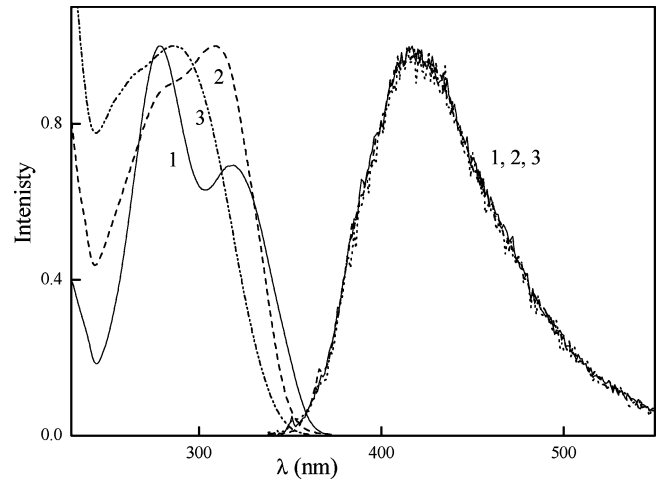

Figure 2. Absorption and emission spectra, obtained under irradiation of the EE, ZE, and ZZ isomers of 1,2-DSB (curves 1, 2, and 3, respectively) in MCH/3MP at room temperature.

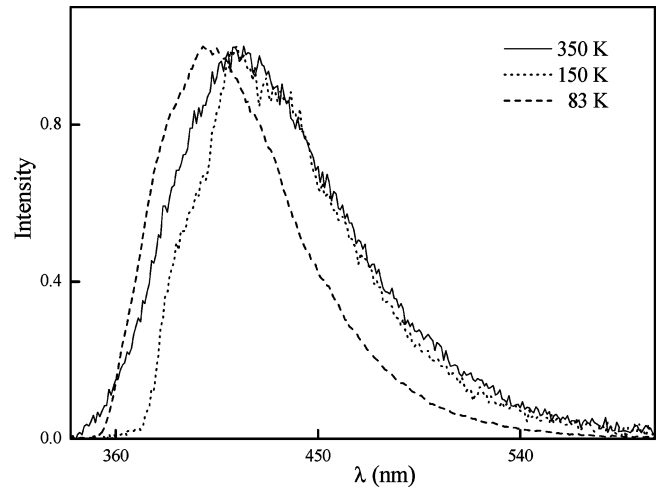

Figure 3. Fluorescence emission spectra of *EE*-1,2-DSB as a function of temperature in MCH/3MP (λ_{exc} = 318 nm).

In the 350−180 K range, the emission spectrum decreases in intensity in the blue region on decreasing temperature; in the 180−120 K temperature range, the spectrum becomes more structured; and below 120 K a progressive spectral shift toward shorter wavelengths can be observed again. These spectral trends indicate that the emission of EE is due to several components whose weight depends on temperature.

In Figure 4, the emission spectra, obtained under irradiation of ZE, are shown as a function of temperature together with those of EE for comparison. In the 350−180 K temperature range, the emission spectra of the two geometrical isomers were found identical, as already observed at room temperature;[16] on the contrary, below 180 K, other emissive components appeared at longer wavelengths, probably due to the ^{1}ZE* rotamers.

Figure 5 shows the absorption and fluorescence excitation spectra of ZE at different temperatures, normalized at the tail of the absorption above 100 K. Because the excitation spectrum never overlapped the corresponding absorption and no λ_{exc} effect was observed on the fluorescence spectra, more than one ZE rotamer have to concur to the absorption but not to the emission.

This result indicates that the ZE rotamers, shown in Chart 1, do not interconvert in the S_1 state, according to the "non-equilibration of excited rotamers" (NEER) principle[23−25] and as expected in the presence of fast ZE → EE photoisomerization (see below). Therefore, at $T > 180$ K, the excitation spectrum,

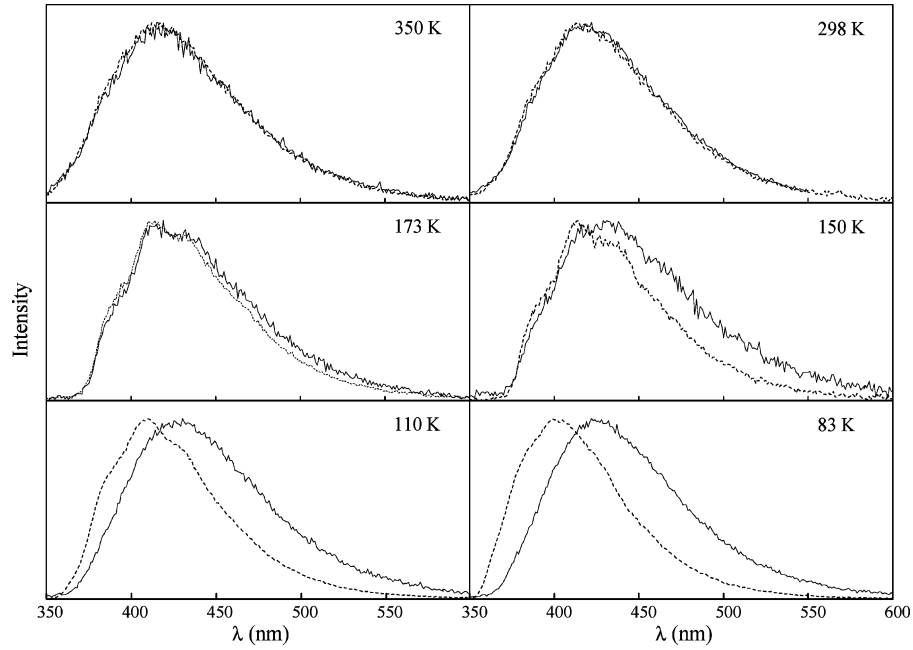

Figure 4. Fluorescence emission spectra obtained under irradiation of *ZE*-1,2-DSB as a function of temperature in MCH/3MP (full lines). The emission spectra of *EE*-1,2-DSB (dotted lines) are shown for comparison (λ_{exc} = 318 nm).

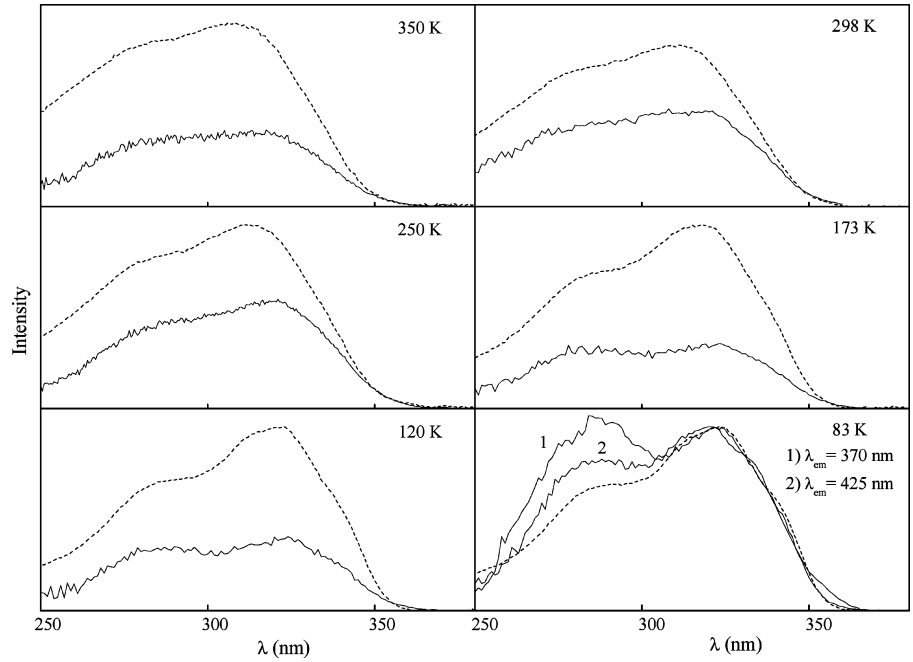

Figure 5. Absorption (dotted lines) and fluorescence excitation (full lines) spectra of *ZE*-1,2-DSB as a function of temperature in MCH/3MP; the excitation spectra were normalized at the tail of the absorption above 100 K (λ_{em} = 425 nm).

whose shape is independent of λ_{em} and temperature, represents the absorption spectrum of a ZE conformer (the B rotamer, see below), which adiabatically produces ^{1}EE*.

Only below 150 K did the excitation and emission spectra of ZE become dependent on λ_{em} and λ_{exc}, respectively, pointing to a multicomponent emission, probably because the intrinsic emissive components from the A and B rotamers of ZE become detectable. This is also in agreement with the calculations that still foresee the presence of both rotamers at low temperatures (an abundance of 75% and 24% is expected for A and B, respectively, in the S_0 state at 83 K).

Also, the spectral trends of the ZZ isomer with temperature were interesting and informative. Figure 6 shows the emission spectra obtained under irradiation of ZE and ZZ in the 295−83 K range. Irradiation of ZZ produced a spectrum that overlapped that obtained exciting either ZE or EE at temperatures above 180 K. Below 170 K, the emission spectrum became similar to that of ZE, showing nevertheless an increase in intensity at the longer wavelengths. These trends confirm the involvement of the adiabatic "one photon-two bonds" processes (^{1}ZZ* → ^{1}ZE* → ^{1}EE*) above 180 K and "one photon-one bond" (^{1}ZZ* → ^{1}ZE*) in the 170−83 K range.

The fluorescence excitation spectrum of ZZ, differently from that of ZE, was found much more similar to the absorption spectrum at each temperature, as expected by the calculations, because the B rotamer is the predominant species even at high temperature.

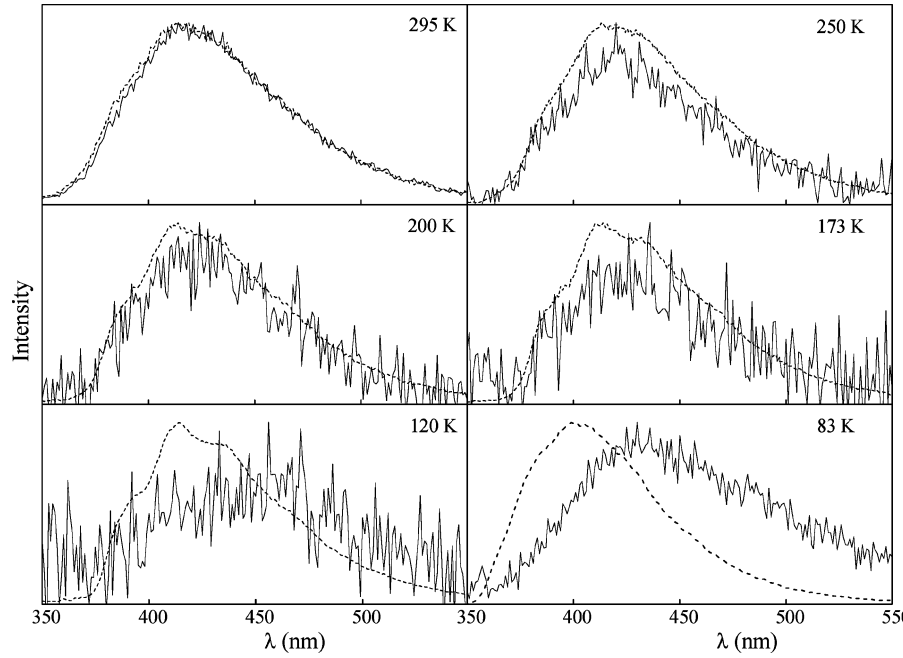

Figure 6. Fluorescence emission spectra measured under irradiation of *ZZ*-1,2-DSB in MCH/3MP as a function of temperature (full lines). The emission spectra of *EE*-1,2-DSB (dotted lines) are shown for comparison (λ_{exc} = 318 nm).

TABLE 2: Fluorescence (ϕ_F) and Photoisomerization ($\phi_{x\rightarrow y}$) Quantum Yields and Fluorescence Lifetimes (τ_F) Obtained under Irradiation of Each Geometrical Isomer (x) of 1,2-DSB in MCH/3MP at Room Temperature

isomer (x)	ϕ_F	τ_F (ns)	$\phi_{x\rightarrow EE}$	$\phi_{x\rightarrow ZE}$
EE	0.37	27		0.05[a]
ZE	0.17	27	0.40[a]	
ZZ	0.04	28	0.08[a]	0.09[a]

[a] From ref 16.

3.2. Photophysical Behavior. The photobehavior of the geometrical isomers of 1,2-DSB in a nonpolar solvent at room temperature was explored and discussed in previous works.[15,16] The measured fluorescence and geometrical photoisomerization quantum yields of these isomers in MCH/3MP at room temperature are resumed in Table 2, together with the fluorescence lifetimes.

It has to be noted that the photoisomerization of the EE isomer is accompanied by non-negligible side photoreactions (a value of 0.15 has been reported for the disappearance quantum yield, ϕ_{EE}^{dis}).[15]

3.2.1. Rotamer Interconversion of EE-1,2-DSB in the S_1 State. The nature of the photoprocesses accompanying isomerization of *EE*-1,2-DSB is a puzzling subject. Primary unstable photoproducts can be in turn implied in photochemical and thermal reactions, such as dimerization, cyclization, and bond cleavage.[26−28] Only in relatively mild conditions (low dose and concentration) was the EE → ZE photoisomerization found to be accompanied by the formation of a compound, assigned to 2,3-diphenyl-2,3-dihydronaphthalene (DDH), formed by cyclization of the compressed geometry of EE (C rotamer),[15] as was also hypothesized in previous works.[26−30]

The study of the temperature effect on the fluorescence parameters (ϕ_F and τ_F) allowed one to confirm that the C rotamer (formed through adiabatic interconversion processes from the elongated A conformer in the S_1 state, against the NEER principle[23−25]) is involved in the relaxation pathways of ^{1}EE*.

Table 3 shows the lifetimes and fluorescence quantum yields of the rotamer mixture of EE as a function of temperature. The fluorescence decay was found to be monoexponential above 140 K (see Figure 7a), and τ_F decreased with increasing temperature, as ϕ_F. Below 140 K, the fluorescence decay became bi- or triexponential (as shown in Figure 7b and c, respectively), and the fluorescence quantum yield of the mixture reached a value of 1, thus revealing the presence of more than one excited species, which decays to the ground state by the radiative process only.

TABLE 3: Temperature Effect on the Fluorescence Parameters of *EE*-1,2-DSB in MCH/3MP (λ_{exc} = 316 nm, λ_{em} = 415 nm)

T (K)	ϕ_F	$\tau_{F,1}$ (ns)	$\tau_{F,2}$ (ns)	$\tau_{F,3}$ (ns)	% (1)	% (2)	% (3)
350	0.15	12.2			100		
330	0.21	17.6			100		
310	0.29	23.5			100		
293	0.37	27.1			100		
250	0.50	28.3			100		
200	0.73	34.5			100		
173	0.75	38.1			100		
150		41.3			100		
140		40.3			100		
130		40.0	4.9		93.5	6.5	
120	0.98	40.1	5.8		90	10	
110		40.7	6.8		88.5	11.5	
83	1.0	36.0	10.0	3.2	68	28	4
40			15.1	5.0		80	20
15			17.1	6.2		70	30
8			17.0	7.0		60	40

The following experimental evidence was obtained: (i) the spectral evolution of the EE absorption with temperature indicates only one absorbing species, the A rotamer, as predicted by calculations; (ii) the emission spectrum is independent of λ_{exc} despite being a combination of several emissive components; (iii) the excitation spectrum, independent of λ_{em}, overlaps the absorption spectrum at all temperatures; (iv) the fluorescence decay is monoexponential above 140 K, whereas it becomes polyexponential at lower temperatures, as previously found in *n*-hexane,[12] with the longest lifetime ($\tau_{F,1}$) independent of temperature (mean value of 39 ns); and (v) the formation of a cyclic compound from ^{1}EE(C)* is observed at room temperature.

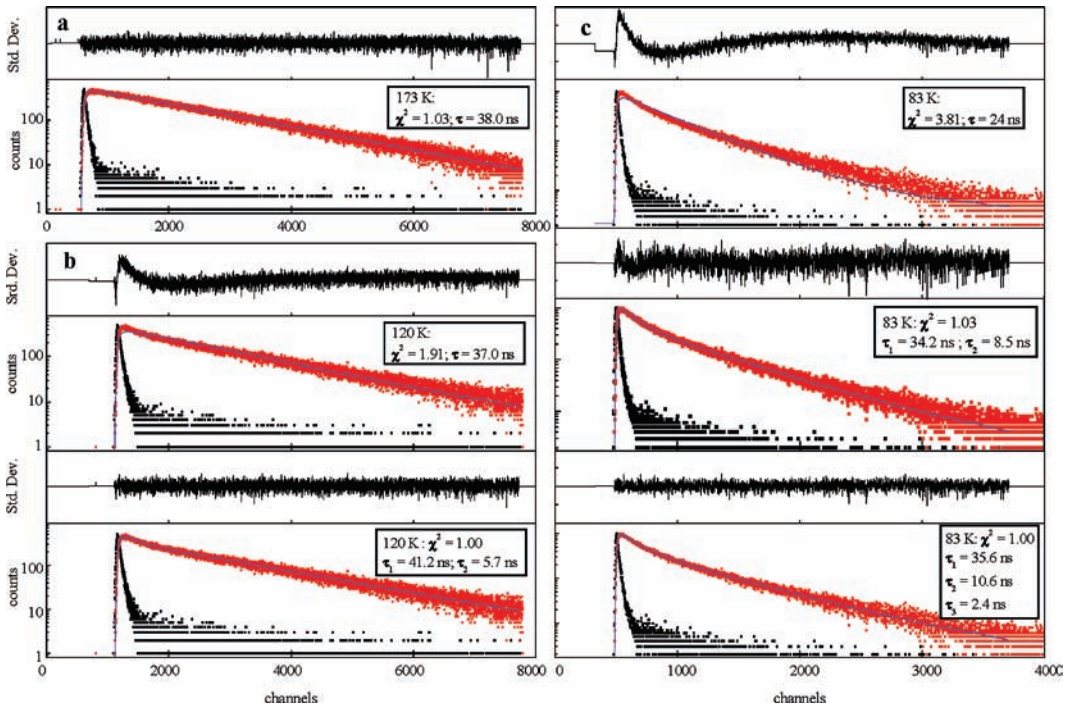

Figure 7. Deconvolution analysis and residuals of the fluorescence decay curves of *EE*-1,2-DSB monitored at 415 nm in MCH/3MP at three temperatures by a mono (a)-, bi (b)-, and tri (c)-exponential treatment.

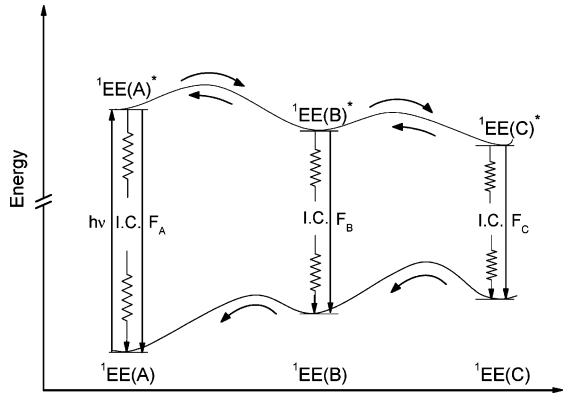

Figure 8. Qualitative sketch of the potential energy curves as a function of rotation around the "quasi-single" bond connecting the styryl moiety to the central benzene ring for the three rotamers of *EE*-1,2-DSB in the S_1 state.

On the basis of these findings, we propose a model (see Figure 8) where only the A rotamer is present in S_0 at all temperatures and consecutive adiabatic interconversions among the excited A, B, and C rotamers of the EE isomer (Chart 1) are operative during their lifetime.

Above 140 K, the three excited rotamers are assumed to be equilibrated (two-way process: ^{1}EE(A)* ↔ ^{1}EE(B)* ↔ ^{1}EE(C)*, equilibrated case) and decay with the same average lifetime, which increases on decreasing temperature, thus suggesting that one or more rotamers have activated steps in the deactivation processes, probably along the reactive ^{1}EE* → ZE and ^{1}EE* → DDH pathways. Below this temperature, the one-way processes ^{1}EE(A)* → ^{1}EE(B)* → ^{1}EE(C)* (total or partial interconversion, nonequilibrated case) become operative, and the fluorescence quantum yield of the rotamer mixture reaches a value of 1, as expected if only rotamer interconversion and fluorescence are involved in the relaxation processes.

On the basis of the trend of the lifetimes with temperature, the longest value ($\tau_{F,1}$) was assigned to the compressed geometry (C rotamer), because it remained practically constant below 160 K, while the shortest ($\tau_{F,3}$) and intermediate ($\tau_{F,2}$) lifetimes were assigned to the elongated (A) and semicompressed (B) rotamer, respectively.

The sketch of the potential-energy curves of the S_1 state, shown in Figure 8, reflects the observed photobehaviors, which obviously depend on the shape of the S_1 energy surfaces as a function of the rotation around the "quasi-single" bonds connecting the styryl moieties to the central benzene ring. The C rotamer should be the most stable species in S_1 also on the basis of the rotamer-specific ^{1}ZZ* → ^{1}ZE* → ^{1}EE* pathways (see below). The inversion of rotamer stability observed in S_1 with respect to that in S_0 is probably due to an electronic reorganization that changes the pattern of single and double bonds.[31]

Examples of interconversion of excited rotamers with or without inversion of their stability in the S_1 state as compared to S_0 were previously reported for 2-vinylanthracene and its β-alkyl derivatives,[32−34] 2-anthrylethenes[35] and 1,3-di-(3′-thienylethenyl)benzene[36] (one-way process), while interconversions followed by re-equilibration among rotamers (equilibrium case) were reported for the trans isomers of 1-(2′-propenyl),2-(2′-anthryl)ethene[37] and *N*-methoxy-1-(2-anthryl)ethanimine.[38]

The increase in the lifetime of the A and B rotamers with decreasing temperature, observed below 130 K (see Table 3), suggests the presence of activated torsional processes, generated by inherent thermal and/or viscosity barriers. To verify the possible involvement of viscosity effect on the excited rotamer interconversion, we measured the fluorescence decay of the EE isomer in P/Hept. This mixture has similar dielectric constant as compared to MCH/3MP but becomes a rigid matrix at 160 K where MCH/3MP is still a fluid solution (glass at ∼110 K). The results obtained on going from a fluid solution ($\eta \cong 0.3$ cP at 293 K) to a rigid matrix at 160 K showed a monoexponential decay above 140 K with lifetime of 25 ns at room temperature and 40 ± 0.3 in the range 180−140 K. Below 140 K, the fluorescence decay became polyexponential with the same trend

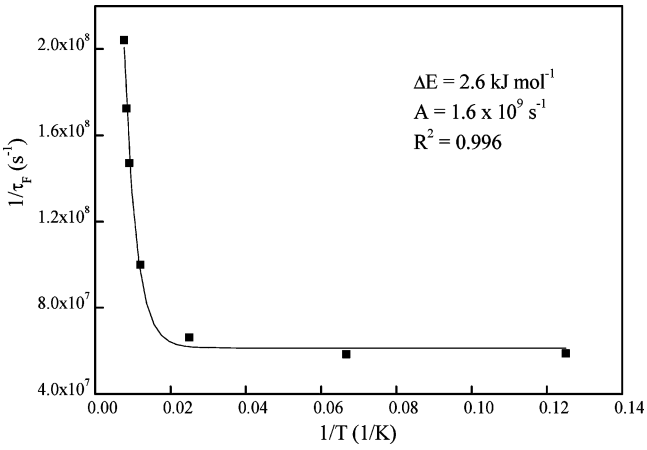

Figure 9. Best fit of the trend of the fluorescence lifetime of the *EE(B)*-1,2-DSB rotamer in MCH/3MP with temperature, according to eq 1.

with temperature as observed in MCH/3MP. These results clearly show that the temperature is the main parameter that controls the rate of the interconversion processes of the EE rotamers in S_1 in nonpolar solvents. This behavior probably indicates that no additional volume is implied in the processes here described. In fact, when the change of geometry demands an increase of volume, as in the case of trans → cis photoisomerization of stilbene, an additional viscosity barrier besides the thermal torsional barrier has to be taken into account in viscous solvents.[39]

Below 130 K (where $\phi_F = 1$), the temperature effect on the fluorescence lifetime of the A and B rotamers allowed one to obtain information on the activated torsional process of their adiabatic interconversions by the Arrhenius-type equation:

$$1/\tau_{F,i(x)} = 1/\tau^{lim}_{F,i(x)} + A \exp(-\Delta E/RT) \quad (1)$$

where i and x represent the geometrical and conformational isomers, respectively, and $\tau^{lim}_{F,i(x)}$ is the lifetime at low temperature, where the activated process is no longer operative, and it is then given by the inverse of the radiative rate constant ($\tau^{lim}_{F,i(x)} = 1/k_{F,i(x)}$), with internal conversion being practically absent. The use of eq 1 implicitly assumes a temperature-independent k_F value. It has to be noted that a change of k_F with temperature was observed for 1,4-DSB[5,12] and some 1,2-diarylethenes,[17,22,40] but k_F of other 1,2-diarylethenes did not show such dependence, even down to a rigid matrix.[17,22] This different behavior is related to the nature of the lowest excited singlet state and/or to the geometry of these flexible molecules. In the present case, the validity of eq 1 in the limited (130−80 K) range is supported by the limiting value reached by τ_F of B and C, which remains constant with decreasing temperature, even if a small effect of temperature on k_F cannot be excluded at higher temperatures.

For the ^{1}EE(B)* → ^{1}EE(C)* process, the best fit of the experimental data according to eq 1 led us to derive the following parameters: $^1\Delta E_{EE(B)^*\rightarrow EE(C)^*} = 2.6 \pm 0.2$ kJ mol^{-1}, $^1A_{EE(B)^*\rightarrow EE(C)^*} = 1.6 \pm 0.4 \times 10^9$ s^{-1}, and $\tau^{lim}_{F,EE(B)} = 16.3$ ns (see Figure 9). The latter is in good agreement with the experimental value of 17 ns. Similar Arrhenius parameters ($^1\Delta E_{EE(B)^*\rightarrow EE(C)^*} = 1.4$ kJ mol^{-1} and $^1A_{EE(B)^*\rightarrow EE(C)^*} = 4.1 \times 10^8$ s^{-1}) were obtained by eq 19 using the experimental value of 17 ns for $\tau^{lim}_{F,EE(B)}$.

Contrary to the ^{1}EE(B)* → ^{1}EE(C)* rotamer interconversion, the activated torsional ^{1}EE(A)* → ^{1}EE(B)* process is competitive with the A fluorescence even at 8 K, thus suggesting that this adiabatic pathway is practically barrierless. From the best fit of the experimental data according to eq 1, the following parameters were roughly estimated: $^1\Delta E_{EE(A)^*\rightarrow EE(B)^*} = 0.75 \pm 0.19$ kJ mol^{-1}, $^1A_{EE(A)^*\rightarrow EE(B)^*} = 4.8 \pm 1.4 \times 10^8$ s^{-1}, and $\tau^{lim}_{F,EE(A)} = 6.7$ ns. These parameters led to rate constants of the torsional process in agreement with the proposed scheme considering also the error in the A lifetime, which could be measured in a limited temperature range (83−8 K).

TABLE 4: Radiative and Rotamer Interconversion Rate Constants (10^7 s^{-1}) of the Three Conformational Isomers of *EE*-1,2-DSB in MCH/3MP at Different Temperatures

rate constant	T (K)	EE(A)	EE(B)	EE(C)
k_F	<130	15	6	2.6
$^1k^{ad}_{EE(x)^*\rightarrow EE(y)^*}$	350	37	44.8	
	170	28	20	
	140	25	14.5	
	110	21	9	
	83	16.2	4.5	
	40	5	0.35	

The rate constants for the adiabatic interconversions, $^1k^{ad}_{EE(x)^*\rightarrow EE(y)^*}$ (where x and y represent the conformers involved), at different temperatures (collected in Table 4 together with the radiative rate constants) were derived from the Arrhenius parameters. For the B* → C* process, the data are the average of the values derived by the two procedures above-described.

The kinetic parameters of the ^{1}EE(A)* → ^{1}EE(B)* process in Table 4 were not derived below 40 K because of the poor reliability of the derived data at lower temperatures.

The values of the radiative rate parameters, derived as $1/\tau^{lim}_{F,i(x)}$, are 15, 6, and 2.6×10^7 s^{-1} at low temperatures for the A, B, and C rotamers, respectively. The k_F value of A is more than twice that of B, just like that of B as compared to C, in agreement with the calculations that predict a similar trend of the oscillator strength for the S_0 → S_1 transition of the EE rotamers. At room temperature, the average value of k_F of the rotamer mixture (1.4×10^7 s^{-1}, derived as $\phi_{F,EE}/\tau_{F,EE}$) results to be one-half of the smallest k_F value calculated at low temperatures (2.6×10^7 s^{-1} for C). This can be due to either uncertainty in the derived parameters and/or a temperature effect on the radiative parameter, which can be valuable at high temperatures only.

Below 100 K, the quantum yield of the excited rotamer interconversion ($^1\phi^{ad}_{EE(x)^*\rightarrow EE(y)^*}$) was calculated at two temperatures by the relationship:

$$^1\varphi^{ad}_{EE(x)^*\rightarrow EE(y)^*}(T) = {}^1k^{ad}_{EE(x)^*\rightarrow EE(y)^*}(T) \times \tau_{F,EE(x)}(T) \quad (2)$$

while the intrinsic contributions of A, B, and C to the fluorescence, $\phi^*_{F,EE(x)}$, were estimated by the following equations:

$$\varphi^*_{F,EE(A)}(T) = [1 - {}^1\varphi^{ad}_{EE(A)^*\rightarrow EE(B)^*}(T)] \quad (3)$$

$$\varphi^*_{F,EE(B)}(T) = [1 - {}^1\varphi^{ad}_{EE(B)^*\rightarrow EE(C)^*}(T)] \times {}^1\varphi^{ad}_{EE(A)^*\rightarrow EE(B)^*}(T) \quad (4)$$

$$\varphi^*_{F,EE(C)}(T) = {}^1\varphi^{ad}_{EE(A)^*\rightarrow EE(C)^*}(T) = ({}^1\varphi^{ad}_{EE(A)^*\rightarrow EE(B)^*} \times {}^1\varphi^{ad}_{EE(B)^*\rightarrow EE(C)^*})(T) \quad (5)$$

The derived parameters are collected in Table 5.

TABLE 5: Fluorescence Contributions ($\phi^*_{F,EE(x)}$) and Adiabatic Interconversion ($^1\phi^{ad}_{EE(x)^*\rightarrow EE(y)^*}$) Quantum Yields of the Rotamers of *EE*-1,2-DSB in MCH/3MP at Different Temperatures

T (K)	$\phi^*_{F,EE(A)}$	$\phi^*_{F,EE(B)}$	$\phi^*_{F,EE(C)}$	$^1\phi^{ad}_{EE(A)^*\rightarrow EE(B)^*}$	$^1\phi^{ad}_{EE(A)^*\rightarrow EE(C)^*}$	$^1\phi^{ad}_{EE(B)^*\rightarrow EE(C)^*}$
83	0.48	0.29	0.23	0.52	0.23	0.45
40	0.75	0.24	0.01	0.25	0.012	0.05

TABLE 6: Temperature Effect on the Fluorescence Parameters Obtained under Irradiation of *ZE*-1,2-DSB in MCH/3MP (λ_{exc} = 318 nm, λ_{em} = 415 nm)

T (K)	ϕ_F	$\tau_{F,1}$ (ns)	$\tau_{F,2}$ (ns)	$\tau_{F,3}$ (ns)	% (1)	% (2)	% (3)
350	0.08	11.4			100		
330	0.12	16.7			100		
310	0.14	22.5			100		
293	0.17	27.0			100		
250	0.26						
200	0.27	36.3			100		
173	0.15	35.2		2.2	92		8
150		33.7		3.0	65		35
140		32.5		3.6	49		51
130			18.1	3.8		36	64
120	0.12		14.4	4.0		30	70
83	0.31		9.0	4.1		65	35

The trend of the emission spectrum of the rotamer mixture with temperature, described in section 3.1, is well explained by the derived parameters of Table 4. Above 150 K, $^1k^{ad}_{EE(x)^*\rightarrow EE(y)^*}$ is about $1/\tau_{F,EE(x)}$, as expected in the case of equilibration of the excited rotamers (two-way process).[19] The emission spectrum is mainly originated from ^{1}EE(C)*, the most abundant species in S_1, with the rotamer contributions to the emission spectrum of the mixture being mainly dependent on the conformer enthalpy differences in S_1. Below 140 K, $^1k^{ad}_{EE(x)^*\rightarrow EE(y)^*}$ is lower than $1/\tau_{F,EE(x)}$ (one-way process[19]): the ^{1}EE(B)* $\rightarrow$ ^{1}EE(C)* process remains competitive with the radiative deactivation above 80 K, in agreement with the trend of the fluorescence spectrum and the presence of the emissive component from ^{1}EE(C)* in the decay curves, whereas the ^{1}EE(A)* $\rightarrow$ ^{1}EE(B)* pathway is still operative at lower temperatures. These results are in agreement with the large increase of the blue components of the fluorescence spectrum, observed at 83 K and due to an increase in the weight of the emission from ^{1}EE(A)* and ^{1}EE(B)*.

3.2.2. Adiabatic Pathways in the Cis → Trans Photoisomerization. The fluorescence lifetimes, measured under irradiation of the compounds bearing cis double bonds at room temperature (Table 2), were assigned to ^{1}EE* adiabatically produced.[16] The EE → ZE photoisomerization was reported to occur with a very low quantum yield (0.05 at room temperature[15]) through the diabatic mechanism ^{1}EE* → ^{1}PE* → ^{1}PE → α ^{1}ZE + (1 − α) ^{1}EE, implying $S_0 \leftarrow S_1$ internal conversion at the perpendicular configuration (^{1}PE*). On the contrary, the geometrical isomerization of the cis (ZE and ZZ) compounds was supposed to involve adiabatic pathways (directly in a unique potential energy surface), without nevertheless considering the role that different conformational isomers of ZE and ZZ could have in the photophysical and photochemical behavior of these compounds.

The results of this work allow one to propose a complete scheme of the deactivation pathways [reactive (conformational and/or geometrical isomerizations), radiative, and radiationless] of the lowest excited singlet state of all of the 1,2-DSB isomers.

3.2.2.1. ZE-1,2-DSB. The fluorescence parameters measured under irradiation of ZE as a function of temperature are collected in Table 6.

Above 180 K, the fluorescence decay was monoexponential with a lifetime just like that observed under irradiation of EE at each temperature (see Table 3), and then $\tau_{F,1}$ was assigned to the rotamer mixture of EE, adiabatically produced by the ^{1}ZE* → ^{1}EE* process. At lower temperatures, the decay became biexponential. The $\tau_{F,2}$ value was reasonably assigned to a rotamer mixture of EE and ZE and practically coincides with $\tau_{ZE(A)}$ in a rigid matrix at 83 K, where the trend of the fluorescence spectrum with temperature showed the lack of the emissive components originated from the EE rotamers. The shortest lifetime ($\tau_{F,3}$), dependent on temperature, was attributed to the ZE(B) conformer, because it is the unique rotamer that can adiabatically isomerize to EE (see below). The adiabatic cis → trans photoisomerization takes place through the classic "one bond flip" mechanism, which produces the geometrical isomer keeping the same conformational geometry: ^{1}ZE(B)* → ^{1}EE(B)*, as found for diarylethenes[40−47] and heteroanalogues of distyrylbenzene.[46,48]

The torsional barrier of this rotamer-specific process was derived by the Arrhenius-type equation:

$$\ln(1/\tau_{F,i(x)} - 1/\tau^{lim}_{F,i(x)}) = \ln A - \Delta E/RT \qquad (6)$$

in the limited temperature range 173−130 K, as shown in Figure 10. The plot in the inset shows a linear trend and led us to derive the following Arrhenius parameters: 1.1×10^{12} s^{-1} and 12.1 kJ mol^{-1} for the frequency factor and energy barrier, respectively. The high value of the A parameter, characteristic of a spin-allowed process, indicates that the photoisomerization proceeds through an activated singlet mechanism. The rate constant of the adiabatic pathway at the explored temperatures was obtained from the Arrhenius parameters. The $^1k^{ad}_{ZE(B)^*\rightarrow EE(B)^*}$ value markedly increases with temperature: from 2.7×10^4 (at 83 K) to 1.8×10^{10} s^{-1} (at 350 K) and assumes the value of 8×10^9 s^{-1} at 293 K. These results show that the activated process is only operative above 120 K and is expected to be the unique deactivation channel of the ^{1}ZE(B)* rotamer above 250 K.

The quantum yield of the rotamer-specific ^{1}i(x)* → ^{1}r(x)* geometrical isomerization at the explored temperatures was

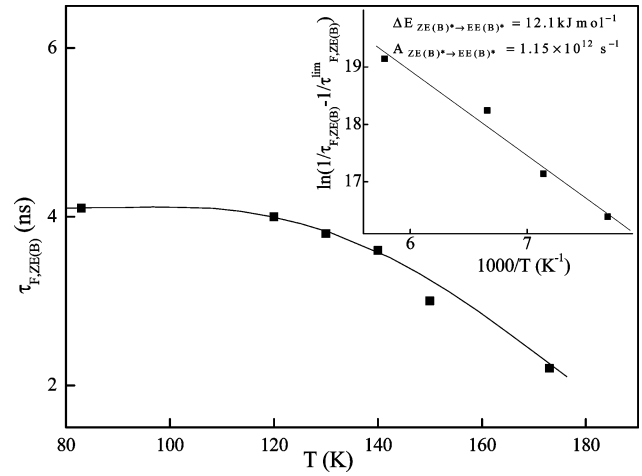

Figure 10. Trend of the fluorescence lifetimes against temperature for the B rotamer of *ZE*-1,2-DSB in MCH/3MP. The inset shows the Arrhenius plot.

derived by the relationship:

$$^{1}\varphi^{ad}_{i(x)^{*}\rightarrow r(x)^{*}}(T) = \varphi_{F,i(x)}/\varphi_{F,EE}(T) \quad (7)$$

In eq 7, $\phi_{F,i(x)}$ is the fluorescence quantum yield, derived for the x rotamer of the i isomer. This parameter was obtained under excitation of the cis (ZE or ZZ) isomer at the temperatures where only the emission from ^{1}EE* was observed. The experimental yield ($\phi_{F,i}$) was then corrected by the quanta absorbed by the x rotamer, involved in the cis → trans isomerization, through the equation:

$$\varphi_{F,i(x)}(T) = \varphi_{F,i}(T)/\%[^{1}i(x)^{*}](T) \quad (8)$$

where $\%[^{1}i(x)^{*}]$ represents the % of quanta absorbed by the i(x) rotamer at λ_{exc}, and $\phi_{F,i}$ is the fluorescence quantum yield, measured under excitation of the i isomer. The $\%[^{1}i(x)^{*}]$ values were estimated by the ratio between the intensities of the excitation and absorption spectra (normalized at their tail) at the same wavelength used for excitation (see Figure 5 for ZE).

By eqs 7 and 8, a value of 1 was obtained for the ^{1}ZE(B)* → ^{1}EE(B)* quantum yield above 250 K, in agreement with the values of $^{1}k^{ad}_{ZE(B)^{*}\rightarrow EE(B)^{*}}$. Below 180 K, $^{1}\phi^{ad}_{ZE(B)^{*}\rightarrow EE(B)^{*}}$ was obtained by eq 9:

$$^{1}\varphi^{ad}_{ZE(B)^{*}\rightarrow EE(B)^{*}}(T) = [^{1}A^{ad}_{ZE(B)^{*}\rightarrow EE(B)^{*}} \exp(-^{1}\Delta E^{ad}_{ZE(B)^{*}\rightarrow EE(B)^{*}}/RT] \times [\tau_{F,ZE(B)}(T)] \quad (9)$$

and its value goes from 0.56 at 173 K to 0.02 at 120 K.

Above 200 K, where equilibration among the EE excited rotamers is operative, the contribution of the ZE(B) → EE(B) adiabatic mechanism in S_1 to the overall ZE → EE isomerization was estimated by the relationship:

$$^{1}\varphi^{ad}_{ZE(B)\rightarrow EE(B)}(T) = [^{1}\varphi^{ad}_{ZE(B)^{*}\rightarrow EE(B)^{*}} \times \%[^{1}ZE(B)^{*}] \times {}^{1}\varphi_{G,EE}](T) \quad (10)$$

where $^{1}\phi_{G,EE} = (1 - \phi^{dis}_{EE})$ is the overall quantum yield of the nonreactive deactivation to the ground state for the EE isomer.

A value of 0.48 was obtained for $^{1}\phi^{ad}_{ZE(B)\rightarrow EE(B)}$ at 293 K. Considering the uncertainty in the measured yield and derived parameters of eq 10, this calculated value can be considered to practically correspond to the measured ZE → EE quantum yield (0.40 at room temperature, see Table 2). This clearly indicates that the photoconversion of ZE takes place through a unique singlet mechanism, implying the rotamer-specific ^{1}ZE(B)* → ^{1}EE(B)* torsional process. These results are resumed in Figure 11, which shows the deactivation processes of the S_1 state of the A and B rotamers of ZE.

3.2.2.2. ZZ-1,2-DSB. The spectral behavior and the photophysical and photochemical properties, obtained under excitation of the ZZ isomer of 1,2-DSB in a nonpolar solvent at room temperature, evidenced the involvement of "one photon-one bond" and "one photon-two bonds" adiabatic pathways in the cis → trans photoisomerization.[16] The quantum yield of the ZZ → ZE and ZZ → EE photoprocesses in S_1 was obtained by relationships analogous to eqs 7 and 10, in which, however, the presence of the ZZ conformers in the ground state and then their possible role in the photoreactive processes was not considered.[16] As previously said, the calculation results and the

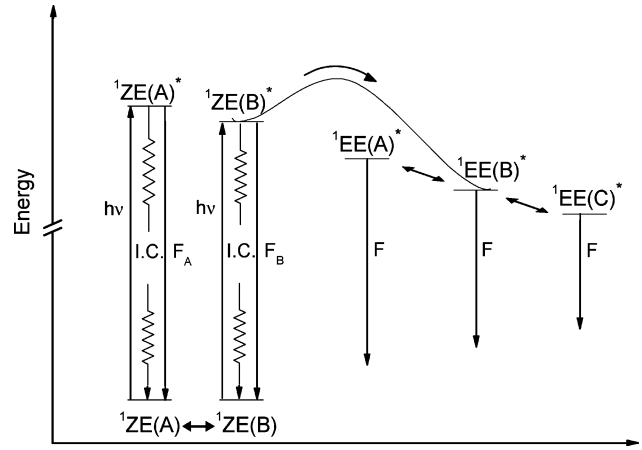

Figure 11. Qualitative sketch of the photoisomerization mechanism of *ZE*-1,2-DSB in MCH/3MP.

TABLE 7: Temperature Effect on the Fluorescence Parameters Obtained under Irradiation of *ZZ*-1,2-DSB in MCH/3MP (λ_{exc} = 316 nm, λ_{em} = 415 nm)

T (K)	ϕ_F	$\tau_{F,1}$ (ns)	$\tau_{F,2}$ (ns)	$\tau_{F,3}$ (ns)[a]	% (1)	% (2)	% (3)
350	0.017	12.0			100		
330	0.022	17.5			100		
310	0.027	24.2			100		
293	0.040	28.1			100		
250	0.038	31.7			100		
200	0.032	30.6			100		
173	0.018	30.0	2.2	(0.3)	86	9	4
150		31.1	3.1	(0.3)	44	43	13
140			3.9	(0.5)		78	22
120	0.008		3.8	(0.4)		83	17
83			4.4	(0.6)		89	11

[a] Values in parentheses are at the limit of the time resolution in our experimental conditions.

trend of the absorption with temperature show that the ZZ geometrical isomer exists in S_0 as a mixture of the A and B rotamers (see Chart 1) (B ca. 92% at room temperature) above 180 K, whereas below this temperature only the B conformer is present.

The fluorescence parameters measured under irradiation of ZZ as a function of temperature are collected in Table 7.

As found for ZE, the trend of the emission spectrum and fluorescence decay with temperature, above 180 K, follows that of the EE isomer (see Table 3). Therefore, $\tau_{F,1}$ was assigned to the rotamer mixture of EE, adiabatically produced by the "one photon-two bonds" ^{1}ZZ* → ^{1}EE* process. At lower temperatures, the decay became polyexponential with $\tau_{F,2}$ assigned to the B rotamer of ZE (on the basis of the same trend of the fluorescence properties with temperature, obtained under excitation of ZE) and $\tau_{F,3}$, practically independent of temperature, to ZZ(B), being the unique rotamer expected for ZZ below 180 K.

All of these findings indicate that conformation plays an important role in the photochemical behavior of ZZ. In fact, the A and B rotamers of ZZ are responsible for the ZZ → ZE (1-fold adiabatic) and ZZ → EE (2-fold adiabatic) isomerizations, respectively.

The sketch of Figure 12 is then proposed for the relaxation processes of the S_1 state of the A and B rotamers of ZZ. They both are present in the S_0 state at $T \geq 140$ K, whereas only the B rotamer exists at lower temperatures.

Above 200 K, the quantum yield of the rotamer-specific ^{1}ZZ(B)* → ^{1}ZE(B)* process at the explored temperatures was

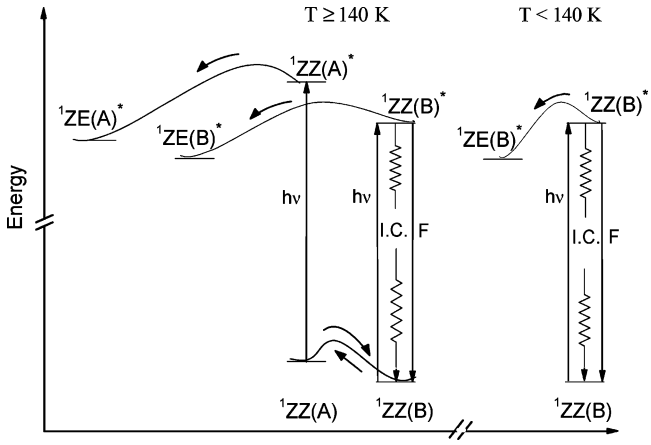

Figure 12. Qualitative sketch of the photoisomerization mechanism of *ZZ*-1,2-DSB in MCH/3MP in two different temperature ranges.

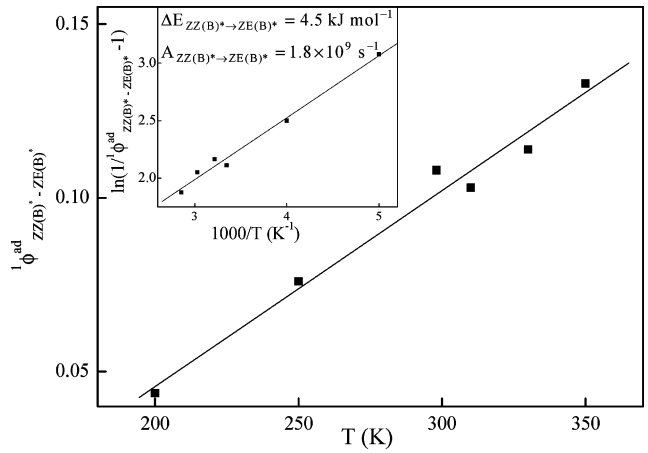

Figure 13. Adiabatic quantum yield of the ^{1}ZZ(B)* → ^{1}ZE(B)* process of *ZZ*-1,2-DSB in MCH/3MP as a function of temperature. The inset shows the Arrhenius plot.

obtained by eqs 7 and 8, with $^1\phi^{ad}_{ZE(B)^* \rightarrow EE(B)^*} \cong 1$. The $^1\phi^{ad}_{ZZ(B)^* \rightarrow ZE(B)^*}$ value goes from 0.13 at 350 K to 0.044 at 200 K and is 0.1 at room temperature. The torsional barrier was then derived by the Arrhenius-type equation:

$$\ln[(1/^1\varphi^{ad}_{ZZ(B)^* \rightarrow ZE(B)^*}) - 1] = \ln(^1A^{ad}_{ZZ(B)^* \rightarrow ZE(B)^*} \times \tau^{lim}_{F,ZZ(B)})^{-1} + (^1\Delta E^{ad}_{ZZ(B)^* \rightarrow ZE(B)^*}/RT) \quad (11)$$

The plot of eq 11 showed a linear trend (see Figure 13) and led us to derive the following Arrhenius parameters for the adiabatic ^{1}ZZ(B)* → ^{1}ZE(B)* process: 1.8×10^9 s^{-1} and 4.5 kJ mol^{-1} for the frequency factor and torsional energy barrier, respectively. The derived $^1k^{ad}_{ZZ(B)^* \rightarrow ZE(B)^*}$ value goes from 3.8×10^8 at 350 K to 2.6×10^6 s^{-1} at 83 K and is 2.8×10^8 s^{-1} at room temperature.

On the basis of Figure 12, the measured ZZ → EE and ZZ → ZE quantum yields of Table 2 can also be expressed by eqs 12 and 13:

$$\varphi_{ZZ \rightarrow EE}(T) = {}^1\varphi^{ad}_{ZZ(B)^* \rightarrow ZE(B)^*} \times {}^1\varphi^{ad}_{ZE(B)^* \rightarrow EE(B)^*} \times {}^1\varphi_{G,EE} \times \%[^1ZZ(B)^*](T) \quad (12)$$

$$\varphi_{ZZ \rightarrow ZE}(T) = {}^1\varphi^{ad}_{ZZ(A)^* \rightarrow ZE(A)^*} \times {}^1\varphi_{G,ZE(A)} \times \%[^1ZZ(A)^*](T) \quad (13)$$

At 293 K, one obtains the $\phi_{ZZ \rightarrow EE}$ value of 0.078 by eq 12, using the derived quantum yields and the values of 0.08 and 0.92 for %[^{1}ZZ(A)*] and %[^{1}ZZ(B)*], respectively. The latter values, which depend on the relative abundance in S_0 and molar absorption coefficient at λ_{exc}, $\varepsilon_{ZZ(x)}(\lambda_{exc})$, were obtained considering their enthalpy difference in the ground state and assuming similar $\varepsilon_{ZZ(x)}$ for the two rotamers of ZZ on the basis of the calculation results (see Table 1). The derived $\phi_{ZZ \rightarrow EE}$ value is in very good agreement with the experimental quantum yield (0.08, see Table 2), thus further supporting the validity of the proposed model for the photobehavior of the three geometrical isomers of 1,2-DSB.

The ZZ → ZE isomerization can only proceed through the adiabatic singlet mechanism involving the rotamer-specific ^{1}ZZ(A)* → ^{1}ZE(A)* process, whose quantum yield can be derived by eq 13, where $^1\phi_{G,ZE(A)} = 1$, because ZE(A) does not photoreact. A value of ~1 was thus derived for $^1\phi^{ad}_{ZZ(A)^* \rightarrow ZE(A)^*}$ at 293 K. At temperatures below 140 K, the fluorescence quantum yield measured by direct excitation of ZZ, $\phi_{F,ZZ}$, is the sum of the contributions from ^{1}ZZ(B)* and its ^{1}ZE(B)* isomeric photoproduct, adiabatically formed. Therefore, it can be expressed by the following relationship:

$$\varphi_{F,ZZ}(T) = \varphi_{F,ZE(B)}(T) \times {}^1\varphi^{ad}_{ZZ(B)^* \rightarrow ZE(B)^*}(T) + \varphi_{F,ZZ(B)}(T) \quad (14)$$

where the intrinsic fluorescence quantum yield of ZZ(B), $\phi_{F,ZZ(B)}$, was calculated by a procedure based on fluorescence decay measurements. The contribution of this species to the experimental $\phi_{F,ZZ}$ value can be obtained by eq 15:

$$\varphi_{F,ZZ(B)}(T) = \%ZZ(B)(\lambda_{em}, T) \times \varphi_{F,ZZ}(T) \quad (15)$$

where % [ZZ(B)], which depends on λ_{em} and temperature, is the weight of the B rotamer in the total fluorescence decay. Its value was roughly derived by the pre-exponential factor of the fluorescence decay, assuming that the ratio of the fluorescence intensities at the wavelength of the emission maximum of the two components is equal to the ratio of their fluorescence quantum yields. This assumption seems to be reasonable because these rotamers have similar and unstructured fluorescence spectra. The value of 0.0014 was derived for $\phi_{F,ZZ(B)}$ at 120 K.

By eqs 14 and 15 and by the equation:

$$\varphi_{F,ZE(B)}(T) = [\varphi_{F,ZE}(T) \times \%ZE(B)(T)]/(\%[^1ZE(B)^*](T)) \quad (16)$$

it was possible to estimate the intrinsic fluorescence quantum yield of ZE(B), $\phi_{F,ZE(B)}$. At 120 K, a mean value of 0.47 ± 0.14 was thus derived, introducing the value of 0.0095 for $^1\phi^{ad}_{ZZ(B)^* \rightarrow ZE(B)^*}$ and the value of 0.27 ± 0.02 for %[^{1}ZE(B)]* in eq 16. The latter value was obtained as the average between those calculated either by the procedure, previously described, which utilizes the absorption and excitation spectra of ZE, or by the rotamer enthalpy difference in S_0, considering the same value for the absorption coefficient of the A and B rotamers at λ_{exc}.

TABLE 8: Measured and Derived Photophysical and Kinetic (10^7 s^{-1}) Parameters of the Rotamers of *ZZ*- and *ZE*-1,2-DSB in MCH/3MP at 120 K

rotamer	ϕ_F	τ_F (ns)	k_F	k_{IC}	$^1k^{ad}_{ZZ(B)^*\rightarrow ZE(B)^*}$	$^1k^{ad}_{ZE(B)^*\rightarrow EE(B)^*}$
ZZ(B)	0.0014	0.5	0.27	200	1.9	
ZE(B)	0.47	4.0	12	12.5		0.5
ZE(A)[a]	0.26	9.0	2.9	8.5		

[a] At 83 K.

The rate parameters of the radiative and $S_0 \leftarrow S_1$ internal conversion, $k_{IC,i(x)}$, processes of the ZZ and ZE rotamers were derived at low temperatures by the equations:

$$k_{F,ZZ(B)} = \varphi_{F,ZZ(B)}/\tau_{F,ZZ(B)} \quad (17)$$

$$k_{F,ZE(B)} = [(\varphi_{F,ZZ} - \varphi_{F,ZZ(B)})/{}^1\varphi^{ad}_{ZZ(B)^*\rightarrow ZE(B)^*}]/\tau_{F,ZE(B)} \quad (18)$$

$$k_{F,ZE(A)} = \{\varphi_{F,ZE} - (k_{F,ZE(B)} \times \tau_{F,ZE(B)} \times \%[{}^1ZE(B)^*])\}/\{\%[{}^1ZE(A)^*] \times \tau_{F,ZE(A)}\} \quad (19)$$

$$k_{IC,i(x)} = 1/\tau_{F,i(x)} - (k_{F,i(x)} + {}^1k^{ad}_{i(x)^*\rightarrow r(x)^*}) \quad (20)$$

Table 8 collects all of the radiative and radiationless decay parameters of S_1 for the rotamers of the ZE and ZZ isomers that are present in the ground state at 120 K, together with their intrinsic photophysical properties.

The radiative rate parameter for ZZ(B) is about 2 orders of magnitude lower than that of the B rotamer of ZE, thus suggesting that the emitting state is a lower-lying forbidden state of A_g parentage, in agreement with the calculation results, which predict an oscillator strength almost 2 orders of magnitude larger for ZE(B). In the case of the ZE isomer, the derived k_F value for the B rotamer is larger than that of A, which has also the highest energy of the $S_0 \rightarrow S_1$ transition. The observed reverse order in both the intensity and the energy for the $S_0 \rightarrow S_1$ transition, as compared to those predicted for these two rotamers by calculations, is not astonishing. In fact, we cannot deny that in the experimental conditions the properties of the two species may undergo small changes leading to slightly different properties with respect to those predicted by the calculations for the isolated molecule.

At low temperatures, the $S_0 \leftarrow S_1$ IC is a relevant deactivation pathway of the S_1 state for the rotamers of ZE and ZZ contrary to the EE rotamers for which the radiative decay is the unique relaxation process below 120 K. In the case of ZZ(B), the IC process is so fast that its lifetime appears to be practically independent of temperature.

The adiabatic ZZ → ZE and ZE → EE isomerizations, specific of the B conformations, are still operative at 120 K, particularly in the case of ZE.

4. Conclusions

Our experimental results, in agreement with MO calculations, show that the conformational geometry of the three geometrical isomers of 1,2-DSB, so far neglected, is a relevant factor in explaining the photoreactivity of these molecules. The EE isomer shows a very different photochemical behavior as compared to that of the cis isomers (ZE and ZZ). In fact, *EE*-1,2-DSB, which exists in the ground state in the elongated geometry (A rotamer) only, undergoes, under irradiation, the adiabatic $^1EE(A)^* \rightarrow {}^1EE(B)^* \rightarrow {}^1EE(C)^*$ rotamer interconversion in the S_1 state in MCH/3MP. Structural factors, reducing the height of the energy barrier for the rotamer interconversion, are probably responsible for the opening of these horizontal pathways by a two-way process (equilibrated case, above 150 K) or by a one-way process (partial interconversion, below 150 K), against the NEER principle.[23−25] As observed in compounds where the excitation energy is largely confined on the aryl group,[49,50] the bonds at the ethene bridge could not undergo the usual reversal of the single/double bond order upon excitation. As a consequence, geometrical isomerization around the double bond is drastically reduced in S_1 ($\phi_{EE\rightarrow ZE} = 0.05$ at room temperature), whereas fast rotamer interconversion around the single bond is operative.

On the contrary, in the case of the ZE and ZZ isomers, different rotamers are present in the S_0 state, which do not interconvert in the excited state, according to the NEER principle. These conformers are then responsible for the adiabatic rotamer-specific cis → trans photoisomerization by singlet mechanism.

Only through an exhaustive study on the spectral and photophysical behaviors of the EE, ZE, and ZZ isomers of 1,2-DSB as a function of temperature, combined with MO calculations, was it possible to understand the photoreaction mechanism of this rather complicated system. The rate parameters of all of the deactivation processes of the excited species were derived, and consequently it was possible to suggest a reasonable model to explain the excited-state properties.

The kinetic treatment showed that: (i) the most stable rotamer of EE in the S_1 state is the compressed C conformer, which is adiabatically produced from $^1EE(A)^*$ even at very low temperatures; (ii) the radiative process is the unique relaxation pathway of all of the EE rotamers below 140 K; (iii) the semicompressed B rotamer of ZE and ZZ is responsible for the adiabatic cis → trans photoisomerization with a quantum yield of ∼1 for the ZE(B) → EE(B) process above 250 K; and (iv) the $S_0 \leftarrow S_1$ internal conversion is a very fast process for ZZ and for the elongated A conformer of ZE.

These results put in evidence that the competition between the horizontal relaxation pathways (conformational and/or geometrical adiabatic isomerization) and the vertical processes (fluorescence and internal conversion) markedly depends on the molecular structure. As a consequence, the temperature and the nature of the lowest excited singlet state of the rotamers are the most important factors in driving the relaxation processes toward the different torsional pathways.

Acknowledgment. This Article is dedicated to our colleagues Professors Giovanna Favaro and Gian Gaetano Aloisi on the occasion of their retirement. We are grateful to Professor Daniele Fioretto and his co-workers (Physics Department of Perugia University) for the use of the cryostat (Cryomech ST405) for liquid helium measurements.

References and Notes

(1) Wang, S.; Oldham, W. J., Jr.; Hudack, R. A., Jr.; Bazan, G. C. *J. Am. Chem. Soc.* **2000**, *122*, 5695–5709.

(2) Segura, J. L.; Martin, N. *J. Mater. Chem.* **2000**, *10*, 2403–2435, and references therein.

(3) Sandros, K.; Sundhal, M.; Wennerstrom, O.; Norinder, U. *J. Am. Chem. Soc.* **1990**, *112*, 3082–3086.

(4) Sundhal, M.; Wennerstrom, O.; Sandros, K.; Arai, T.; Tokumaru, K. *J. Phys. Chem.* **1990**, *94*, 6731–6734.

(5) Marri, E.; Pannacci, D.; Galiazzo, G.; Mazzucato, U.; Spalletti, A. *J. Phys. Chem. A* **2003**, *107*, 11231–11238.

(6) Marri, E.; Elisei, F.; Mazzucato, U.; Pannacci, D.; Spalletti, A. *J. Photochem. Photobiol. A: Chem.* **2006**, *177*, 307–313.

(7) Itoh, Y.; Uozu, Y.; Dote, T.; Ueda, M.; Matsuura, T. *J. Am. Chem. Soc.* **1988**, *110*, 189–198.

(8) Giglio, L.; Mazzucato, U.; Musumarra, G.; Spalletti, A. *Phys. Chem. Chem. Phys.* **2000**, *2*, 4005–4012.

(9) Marri, E.; Galiazzo, G.; Mazzucato, U.; Spalletti, A. *Chem. Phys.* **2005**, *312*, 205–211.

(10) Bartocci, G.; Ginocchietti, G.; Mazzucato, U.; Spalletti, A. *Chem. Phys.* **2006**, *328*, 275–283.

(11) Meier, H. *Angew. Chem., Int. Ed. Engl* **1992**, *31*, 1399–1540, and references therein.

(12) Oelkrug, D.; Rempfer, K.; Prass, E.; Meier, H. *Z. Naturforsch.* **1988**, *43a*, 583–590.

(13) Marri, E.; Galiazzo, G.; Spalletti, A. *Photochem. Photobiol. Sci.* **2004**, *2*, 205–210.

(14) Ginocchietti, G.; Galiazzo, G.; Mazzucato, U.; Spalletti, A. *Photochem. Photobiol. Sci.* **2005**, *4*, 547–553.

(15) Ciorba, S.; Galiazzo, G.; Mazzucato, U.; Sindler-Kulyk, M.; Skoric, I.; Spalletti, A. *J. Photochem. Photobiol. A: Chem.* **2007**, *187*, 325–331.

(16) Ciorba, S.; Bartocci, G.; Galiazzo, G.; Mazzucato, U.; Spalletti, A. *J. Photochem. Photobiol. A: Chem.* **2008**, *195*, 301–306.

(17) Bartocci, G.; Masetti, F.; Mazzucato, U.; Spalletti, A.; Baraldi, I.; Momicchioli, F. *J. Phys. Chem.* **1987**, *91*, 4733–4743.

(18) Mazzucato, U.; Momicchioli, F. *Chem. Rev.* **1991**, *91*, 1679–1719.

(19) Bartocci, G.; Spalletti, A.; Mazzucato, U. In *Conformational Analysis of Molecules in Excited States*; Waluk, J., Ed.; Wiley−VCH: New York, 2000; Chapter 5 and references therein.

(20) Ogawa, K.; Suzuki, H.; Futakami, M. *J. Chem. Soc., Perkins Trans. 2,* **1988**, 39–43.

(21) Marconi, G.; Bartocci, G.; Mazzucato, U.; Spalletti, A.; Abbate, F.; Angeloni, L.; Castellucci, E. *Chem. Phys.* **1995**, *196*, 383–393.

(22) Bartocci, G.; Spalletti, A.; Becker, R. S.; Elisei, F.; Floridi, S.; Mazzucato, U. *J. Am. Chem. Soc.* **1999**, *121*, 1065–1075.

(23) Havinga, E. *Experientia* **1973**, *29*, 1181–1193.

(24) Vroegop, P. J.; Lugtenburg, J.; Havinga, E. *Tetrahedron* **1973**, *29*, 1393–1398.

(25) Jacobs, H. J. C.; Havinga, E. *Adv. Photochem.* **1979**, *11*, 305–373.

(26) Dietz, F.; Scholz, M. *Tetrahedron* **1968**, *24*, 6845–6849.

(27) Laarhoven, W. H.; Cuppen, Th. J. H. M.; Nivard, R. J. F. *Recl. Trav. Chim. Pays-Bas* **1968**, *87*, 687–698.

(28) Laarhoven, W. H.; Cuppen, Th. J. H. M.; Nivard, R. J. F. *Tetrahedron* **1970**, *26*, 1069–1083, and references therein.

(29) Laarhoven, W. H. *Recl. Trav. Chim. Pays-Bas* **1983**, *102*, 241–254.

(30) Laarhoven, W. H. *Pure Appl. Chem.* **1984**, *56*, 1225–1240.

(31) Olivucci, M.; Robb, M. A.; Bernardi, F. In *Conformational Analysis of Molecules in Excited States*; Waluk, J., Ed.; Wiley−VCH: New York, 2000; p 237.

(32) Flom, S. R.; Nagarajan, V.; Barbara, P. F. *J. Phys. Chem.* **1986**, *90*, 2085–2092.

(33) Arai, T.; Karatsu, T.; Sakuragi, H.; Tokumaru, K.; Tamai, N.; Yamazaki, I. *Chem. Phys. Lett.* **1989**, *158*, 429–434.

(34) Arai, T.; Karatsu, T.; Sakuragi, H.; Tokumaru, K.; Tamai, N.; Yamazaki, I. *J. Photochem. Photobiol. A: Chem.* **1992**, *65*, 41–51.

(35) Karatsu, T.; Itoh, H.; Yoshikawa, N.; Kitamura, A.; Tokumaru, K. *Bull. Chem. Soc. Jpn.* **1999**, *72*, 1837–1849.

(36) Bartocci, G.; Ginocchietti, G.; Mazzucato, U.; Spalletti, A. *Chem. Phys.* **2006**, *328*, 275–283.

(37) Bearley, A. M.; Flom, S. R.; Nagarajan, V.; Barbara, P. F. *J. Phys. Chem.* **1986**, *90*, 2092–2099.

(38) Faruuchi, H.; Arai, T.; Sakuragi, H.; Tokumaru, K.; Nishimura, Y.; Yamazaki, I. *J. Phys. Chem.* **1991**, *95*, 10322–10325.

(39) Saltiel, J.; D'Agostino, J. T. *J. Am. Chem. Soc.* **1972**, *94*, 6445–6456.

(40) Bartocci, G.; Spalletti, A.; Mazzucato, U. *Res. Chem. Intermed.* **1995**, *21*, 735–747.

(41) Saltiel, J.; Tarkalanov, N.; Sears, D. F., Jr. *J. Am. Chem. Soc.* **1995**, *117*, 5586–5587.

(42) Spalletti, A.; Bartocci, G.; Elisei, F.; Mancini, V.; Mazzucato, U. *J. Chem. Soc., Faraday Trans.* **1997**, *93*, 211–219.

(43) Spalletti, A.; Bartocci, G. *Phys. Chem. Chem. Phys.* **1999**, *1*, 5623–5632.

(44) Karatsu, T.; Itoh, H.; Nishigaki, A.; Fukui, K.; Kitamura, A.; Matsuo, S.; Misawa, H. *J. Phys. Chem. A* **2000**, *104*, 6993–7001.

(45) Saltiel, J.; Krishnamoorthy, G.; Sears, D. F., Jr. *Photochem. Photobiol. Sci.* **2003**, *2*, 1162–1168.

(46) Bartocci, G.; Mazzucato, U.; Spalletti, A. *Trends Phys. Chem.* **2007**, *12*, 1–36.

(47) Bartocci, G.; Galiazzo, G.; Marri, E.; Mazzucato, U.; Spalletti, A. *Inorg. Chim. Acta* **2007**, *360*, 961–969.

(48) Spalletti, A. *Photochem. Photobiol. Sci.* **2004**, *3*, 695–699.

(49) Momicchioli, F.; Baraldi, I.; Fischer, E. *J. Photochem. Photobiol. A: Chem.* **1989**, *48A*, 95–107.

(50) Bartocci, G.; Masetti, F.; Mazzucato, U.; Spalletti, A.; Orlandi, G.; Poggi, G. *J. Chem. Soc., Faraday Trans. 2* **1988**, *84*, 385–399.

JP903851X